Magneto-transport and exchange biasing in La–Ca–Mn–O compositionally modulated ferromagnetic/antiferromagnetic multilayers

I. Panagiotopoulos
Institute of Materials Science, National Center for Scientific Research ''Demokritos,'' 153 10 Aghia Paraskevi Athens, Greece

C. Christides[a)]
Department of Engineering Sciences, School of Engineering, University of Patras, 26 110 Patras, Greece

D. Niarchos and M. Pissas
Institute of Materials Science, National Center for Scientific Research ''Demokritos,'' 153 10 Aghia Paraskevi Athens, Greece

(Received 23 November 1999; accepted for publication 7 January 2000)

Compositionally modulated structures consisting of $La_{2/3}Ca_{1/3}MnO_3$ ferromagnetic (FM) layers and $La_{1/3}Ca_{2/3}MnO_3$ antiferromagnetic (AF) layers, with layer thickness 1.5 nm $\leqslant t_{FM}, t_{AF} \leqslant 6$ nm, were grown on (100)$LaAlO_3$ by pulsed laser deposition. Thermomagnetic and isothermal magnetic measurements reveal an exchange-biasing mechanism with the same blocking temperature $T_B \approx 70$ K for all the examined combinations of t_{FM} and t_{AF}. The ratio of colossal magnetoresistance increases in multilayers with larger t_{FM}, whereas the exchange-biasing field increases in samples with larger t_{AF}. The independence of T_B on t_{FM} and t_{AF} shows that the artificially induced $La_{1-x}Ca_xMnO_3$ ($x \approx 0.5$) compositional modulation at the interfaces is of critical importance for exchange biasing in La–Ca–Mn–O based multilayers. © *2000 American Institute of Physics.* [S0021-8979(00)01708-4]

I. INTRODUCTION

Several recent studies have focused on mixed valence manganite based artificial superstructures.[1–9] The magnetic and transport properties of these structures are not a simple superposition of the response of the individual layers as interface scattering,[1,2] interlayer interactions,[3,4] and strain-driven effects due to lattice mismatch at interfaces[1,5] modify their magneto-transport properties considerably.

Lately, we have reported[9] the existence of exchange biasing on La–Ca–Mn O multilayers with alternating layers of ferromagnetic (FM) $La_{2/3}Ca_{1/3}MnO_3(\Lambda/2)$ and antiferromagnetic (AF) $La_{1/3}Ca_{2/3}MnO_3(\Lambda/2)$ compositions[10,11] (Λ is the bilayer thickness) grown either on (001)$LaAlO_3$ or (001)$SrTiO_3$ single crystals. Both structural and chemical compatibility between the employed AF and FM layers were important for the coherent growth of atomically perfect interfaces that allowed the development of exchange biasing at low temperatures. The maximum exchange biasing field (H_{EB}) was observed for multilayers grown on top of (001)$LaAlO_3$. In comparison, high quality $[La_{0.6}Sr_{0.4}MnO_3(FM)/La_{0.6}Sr_{0.4}FeO_3(AF)]_{20}$ superlattices, grown on (001)$SrTiO_3$, have shown[3] that the AF spin arrangement in the AF layers can modify the FM spin arrangement in adjacent FM layers but exchange biasing is not reported.

The above results indicate that significant changes occur in the magneto-electronic properties at the interfaces, arising from the competition between the magnetic ordering structures. Specifically, the physics involved in exchange biased[12,13] FM/AF perovskite contacts focuses on the mechanism that leads to a *unidirectional* anisotropy as the double exchange switches to superexchange coupling[14,15] between juxtaposed FM and AF atomic layers. Thus the strength of spin coupling at the AF/FM interfaces, relative to their exchange coupling with spins inside the FM or AF layers, seems to be essential for the exchange biasing mechanism in these heterostructures. Here we investigate the interface related mechanism of spin coupling in $[La_{1/3}Ca_{2/3}MnO_3(t_{AF})/La_{2/3}Ca_{1/3}MnO_3(t_{FM})]_{15}$ multilayers. The experimental results reveal that the exchange-biasing strength and the colossal mangetoresistance (CMR) effect can be engineered by varying independently the AF (t_{AF}) and FM (t_{FM}) layer thicknesses.

II. EXPERIMENTAL DETAILS

Thin films were prepared by pulsed-laser deposition (PLD) of bulk stoichiometric $La_{2/3}Ca_{1/3}MnO_3$ (FM) and $La_{1/3}Ca_{2/3}MnO_3$ (AF) targets on (001)$LaAlO_3$ single crystal substrates. The targets were prepared by standard solid state reaction from La_2O_3, $CaCO_3$ and MnO_2 powders sintered at 1325 °C for five days with two intermediate grindings. The beam of an LPX105 eximer laser (Lambda Physic), operating with KrF gas ($\lambda = 248$ nm), was focused on a rotating target. In order to grow a multilayer structure, the AF and FM targets were mounted on a step-motor controlled rotatable carrier that allows different targets to be sequentially exposed in the beam path. The pulse energy was 225 mJ and the fluence on the target of 1.5 J/cm^2. The substrate was located at a distance of 6 cm from the target, by the edge of

a)Author to whom correspondence should be addressed; electronic mail: christides@ims.demokritos.gr

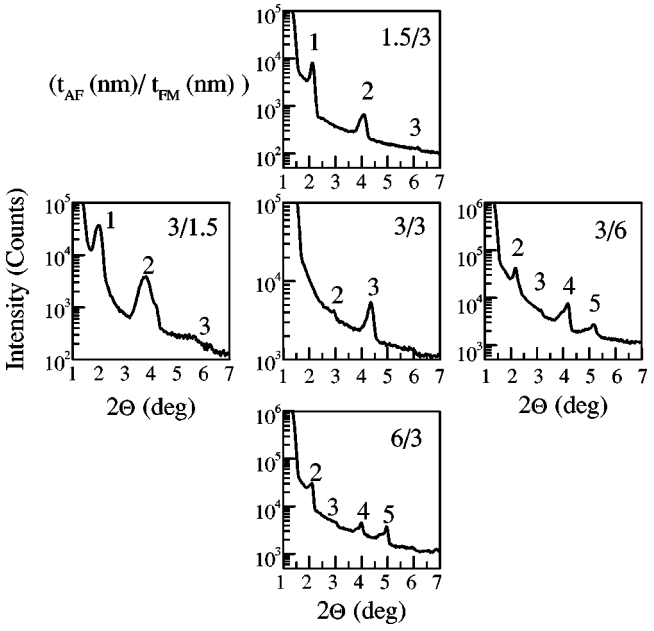

FIG. 1. Low-angle XRD patterns of the $[La_{1/3}Ca_{2/3}MnO_3(t_{AF})/La_{2/3}Ca_{1/3}MnO_3(t_{FM})]_{15}$ multilayers. The t_{AF} and t_{FM} layer thicknesses, in nm units, are indicated as t_{AF}/t_{FM}. The order of the superlattice peaks is shown.

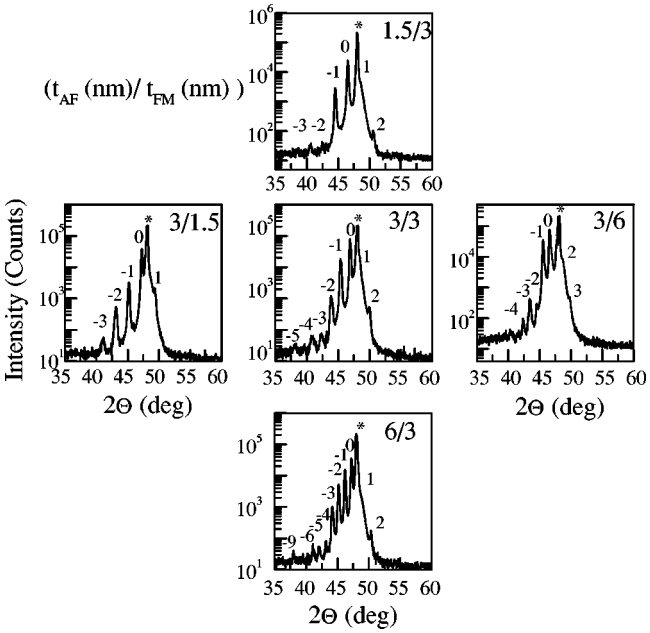

FIG. 2. XRD satellite peaks of the AF/FM multilayers located nearby the (002)$LaAlO_3$ Bragg peak (star). The t_{AF} and t_{FM} layer thicknesses, in nm units, are indicated as t_{AF}/t_{FM}. The order of the satellite peaks is shown.

the visible extent of the plume. During deposition the substrate temperature was stabilized at 700 °C and the oxygen pressure in the chamber was 0.3 Torr, resulting in a deposition rate of 0.03 nm per pulse. Two series of $[La_{1/3}Ca_{2/3}MnO_3(t_{AF})/La_{2/3}Ca_{1/3}MnO_3(t_{FM})]_{15}$ multilayers were deposited on 40-nm-thick AF buffer layer with variable AF/FM compositions. One series is grown with constant $t_{AF}=3$ nm while $t_{FM}=1.5$, 3, 4.5, 6 nm and the other with constant $t_{FM}=3$ nm while $t_{AF}=1.5$, 3, 4.5, 6 nm. To keep every FM layer sandwiched between two AF layers the top layer was AF in all multilayers. For brevity, we named the samples by the ratio t_{AF}/t_{FM} used.

X-ray diffraction (XRD) spectra were collected at ambient conditions with a Siemens D500 diffractometer using Cu $K\alpha$ radiation. Magnetic measurements were performed in a Quantum Design MPMSR2 superconducting quantum interference device (SQUID) magnetometer, with the field applied in the film plane. The magneto-transport measurements have been carried out with the standard four-point probe method, applying the magnetic field parallel to current flow direction.

III. RESULTS

A. X-ray diffraction

The existence of the superstructure is confirmed by the presence of low-angle superlattice Bragg peaks (Fig. 1) and multiple satellite peaks around the (001), (002) and (003) Bragg reflections (Fig. 2). Figure 1 shows that the multilayer with $t_{AF}=t_{FM}=3$ nm (3/3) exhibits zero Bragg intensity at the second order ($m=2$) satellite peak position, whereas for the rest of the samples the intensities of the third order ($m=3$) satellites are suppressed. This provides unambiguous evidence for the accuracy of the selected layer thickness. Specifically, if homogeneous AF and FM layers with constant scattering amplitude densities ϕ_{FM} and ϕ_{AF} are assumed, then the structure factor $F(\theta_m)$ of the mth order Bragg peak, at the low-angle position θ_m is[16]

$$F(\theta_m)=\frac{\Lambda}{\pi m}\sin\left\{\frac{m\pi t_X}{\Lambda}\right\}(\phi_{FM}-\phi_{AF})\Rightarrow,$$

$$F(\theta_m)=0\begin{cases}\text{if } t_X=\Lambda/2 \text{ and } m=2,4,\text{even}\\ \text{if } t_X=\Lambda/3 \text{ and } m=3,6,9,\ldots\end{cases} \tag{3.1}$$

with $t_X=t_{AF}$ or t_{FM}. The medium and high angle XRD patterns (Fig. 2) exhibit intense (00ℓ) Bragg peaks for $\ell=1$, 2, 3, indicating a strong texture along the pseudocubic (001)$LaAlO_3$ direction. Since for all the examined samples there are no traces of mixed (001) and (110) textures then cumulative roughness effects, that may give rise to extra surface roughness and mosaic spread[17] with increasing Λ, can be excluded. The grouping of the satellite peaks observed (Fig. 2) nearby the (002) Bragg position of the $LaAlO_3$ substrate indicates that there is a coherent AF/FM superlattice. Remarkably, a multiplet of asymmetric peak intensities appears around the zeroth order (002) peak of the multilayer. Such an asymmetric intensity of the satellite peaks has been reported in multilayers that exhibit chemical and/or strained interfacial profiles along the growth direction.[18]

Reliable values of Λ have been experimentally estimated from the peak positions in Fig. 2 and are tabulated in Table I. The maximum deviation from the nominal values is about 5%. A 100-nm-thick FM layer, prepared under the same conditions with the multilayers, exhibits a pseudocubic lattice constant $\alpha_p(FM)=0.394$ nm, whereas a 100-nm-thick AF layer exhibits an $\alpha_p(AF)=0.381$ nm. The position of the fundamental ($m=0$) peak in Fig. 2 is used for the estimation

TABLE I. Summary of structural and magnetic parameters. The t_{AF} and t_{FM} layer thicknesses, in nm units, are indicated as t_{AF}/t_{FM}.

t_{AF}/t_{FM}	Λ (nm)	α_p (nm)	H_C(ZFC)(Oe)	H_C(FC)(Oe)	H_{EB} (Oe)
3/1.5	4.6	0.3844	150	400	150
3/3	6.2	0.3872	420	830	300
3/4.5	7.4	0.3886	550	800	270
3/6	9.3	0.3895	670	800	260
1.5/3	4.7	0.3895	510	830	210
3/3	6.2	0.3872	420	830	300
4.5/3	7.7	0.3852	600	920	370
6/3	9.2	0.3864	570	900	540

of the average multilayer lattice constants α_p of a pseudocubic cell. They vary between (Table I) $\alpha_p = 0.3846$ and 0.3896 nm, depending on t_{AF} and t_{FM}.

B. Magnetic measurements

The coercive and exchange biasing fields were derived from isothermal loops at 10 K after zero field cooling (ZFC) from 300 K and field cooling (FC) in 50 kOe. Typical FC and ZFC loops are shown in Fig. 3 for the 6/3 sample. The ZFC loop is symmetric around zero, whereas the FC loop is shifted towards negative fields, evidencing exchange biasing mechanism. A similar loop shift was observed when the sample was measured at a maximum field of 10 kOe. However, the maximum field of 50 kOe was chosen in order to ensure that the measurement does not represent a minor loop. The exchange biasing field H_{EB} can be defined as the loop shift and the coercivity as the half width of the loop. Thus, if H_1 is the lower and H_2 is the higher field value where the average film magnetization becomes zero, then $H_{EB} = -(H_1+H_2)/2$ and $H_c = (H_1-H_2)/2$. The obtained H_c values from the ZFC loops and the H_{EB}, H_c values from the FC loops are given in Table I.

For fixed $t_{FM} = 3$ nm a systematic increase of H_{EB} is observed as the t_{AF} increases and the exchange anisotropy mechanism becomes more effective.[12,19,20] All the FC-H_c values are increased by about 300 Oe relative to the corresponding ZFC-H_c values. Such an increase of H_c, related to the development of the exchange anisotropy, has been reported in several transition metal AF/FM layers.[12,20] However, for fixed $t_{AF} = 3$ nm there is a drastic increase of coercivity in the ZFC loops as t_{FM} is increased from 1.5 to 6 nm. This can be attributed to structural changes, due to strain-driven effects in coherently grown interfaces.[21]

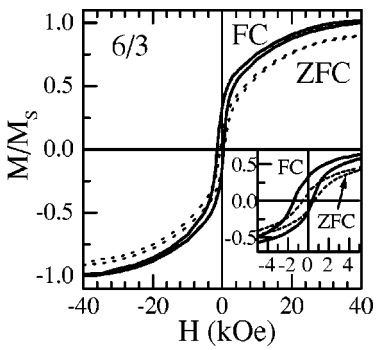

FIG. 3. Magnetic hysteresis loops, measured at 10 K after ZFC from 300 K (dotted line) and FC (solid line) in 50 kOe, for the 6/3 sample. The inset shows an enlargement of the low field data to demonstrate the loop shift.

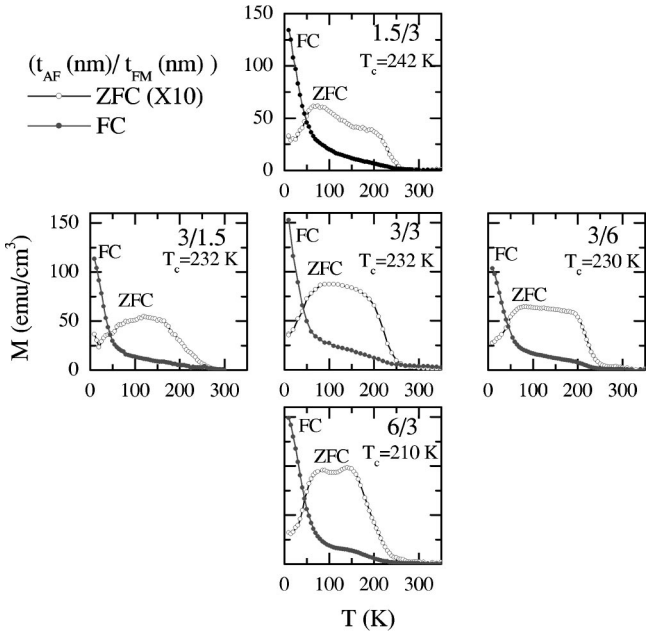

FIG. 4. ZFC and FC magneto-thermal measurements performed in a field of 100 Oe. The t_{AF} and t_{FM} layer thicknesses, in nm units, are indicated as t_{AF}/t_{FM}. Magnetization is normalized to the total FM volume of the sample. The ZFC values are multiplied by a factor of 10 for clarity.

Although the H_{EB} (Table I) varies monotonically with t_{AF} for fixed $t_{FM} = 3$ nm, there is a significant reduction of H_{EB} in the 3/1.5 sample when t_{FM} varies with fixed $t_{AF} = 3$ nm. Such deviations from the expected $H_{EB} \sim 1/t_{FM}$ monotonic relation have been observed in several cases when t_{FM} becomes very thin.[12,22,23] Also it is worth noting that the FC-H_c values are very different from the ZFC ones, following the dependence of H_{EB} on t_{FM}. This reveals a connection between the coercivity and the exchange biasing mechanisms. Thus, the H_{EB} and t_{FM} values in Table I can provide an estimation of the unidirectional interfacial energy: $\Delta E = M_S H_{EB} t_{FM}$. The ΔE is estimated to be in the range of 0.01–0.1 erg/cm^2 and is comparable with energies reported in other AF/FM systems.[12]

Figure 4 shows the magneto-thermal ZFC and FC curves for all the multilayered samples. Both measurements were performed by warming up in 100 Oe after having cooled in zero field and 100 Oe, respectively. The ZFC values have been multiplied by a factor of 10 for clarity. The ZFC and FC curves are characterized by very distinct features: (i) The FC curve exhibits a steep increase below 70 K, that defines[9] a blocking temperature T_B due to alignment of interfacial magnetic moments.[24] (ii) The ZFC curves exhibit a plateau region between $T_B \leqslant T \leqslant T_c$ and the magnetization tends to zero at the T_c of the FM layers. The observed drop of ZFC magnetization below the T_B has been explained[9] by a thermally activated magnetic rotation (thermal remagnetization) over energy barriers caused by random exchange coupling at the AF/FM interfaces. Thus the magnetic order of the multilayers is determined mainly by the interfacial spin ordering.

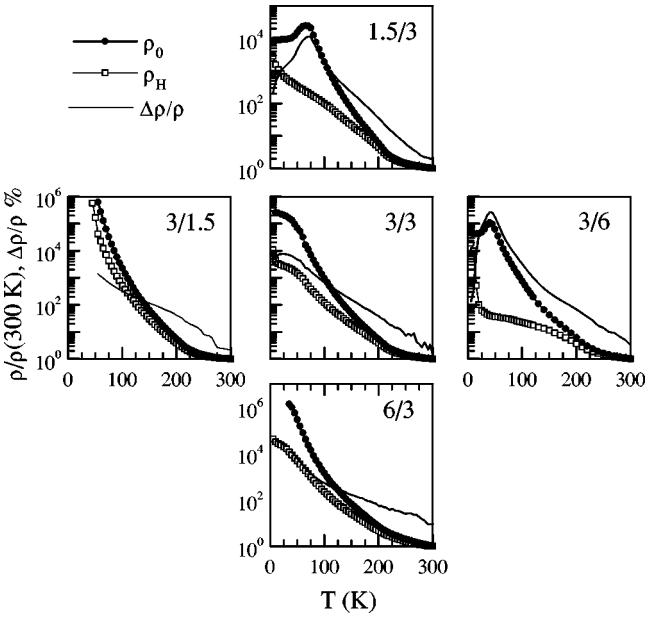

FIG. 5. ZFC and FC temperature variation of resistivity $\rho(T)$ normalized to the $\rho(300\ \mathrm{K})$ value observed at 300 K. The t_{AF} and t_{FM} layer thicknesses, in nm units, are indicated as $t_{\mathrm{AF}}/t_{\mathrm{FM}}$. The CMR ratio $\Delta\rho/\rho_H=[\rho_0-\rho_H]/\rho_H$ is plotted as a solid line.

The displayed T_c values in Fig. 4 were estimated by extrapolating the linear part of M^2 vs T curves near the transition point.[25] Remarkably, the T_c decreases for thicker t_{AF}, indicating that magnetic frustration is induced in the FM layers[3] due to enhancement of the exchange biasing effects (Table I) at the AF/FM interfaces as t_{AF} increases. Accordingly, the $t_{\mathrm{FM}}/3$ series does not exhibit a significant variation of the T_c as a function of t_{FM}.

C. Magneto-transport properties

Figure 5 shows the temperature variation of the normalized resistivity, measured in 50 kOe (ρ_H) and in zero applied field (ρ_0). The $\Delta\rho/\rho_H=[\rho_0-\rho_H]/\rho_H$ ratio (solid line) gives an estimate of the CMR effect. The resistivity increases steeply by cooling down, spanning several orders of magnitude between 300 and 5 K. This is due to the presence of the insulating AF layers of $La_{1/3}Ca_{2/3}MnO_3$ within the multilayered structure.[26] Characteristically, the resistance in 3/1.5 and 6/3 samples becomes so high that it cannot be measured accurately at low temperatures. Thus the increase of resistivity is more drastic in samples with thicker t_{AF} because the insulating behavior of the AF layers masks the transport properties of the FM layers and FM/AF interfaces. Moreover, samples with $t_{\mathrm{AF}}<t_{\mathrm{FM}}$ (like the 1.5/3 and 3/6) exhibit a peak around the T_B, revealing a strong contribution from interfacial spin alignment. Accordingly, the maximum of the resistivity peak occurs around the T_B, where the most drastic change of thermal magnetization appears (Fig. 4), and not around the T_c. Thus samples with $t_{\mathrm{AF}}<t_{\mathrm{FM}}$ exhibit larger CMR ratios than samples with $t_{\mathrm{AF}}>t_{\mathrm{FM}}$, where the difference between ρ_0 and ρ_H is small.

IV. DISCUSSION AND CONCLUSIONS

The present study reveals that, generally, there are two important issues associated with exchange-biased CMR-manganite multilayers. The first refers to the physical origin of the exchange biasing mechanism itself and, second, the observed independence of T_B on t_{AF} or t_{FM}. A recent study[3] in high-quality $La_{0.6}Ca_{0.4}MnO_3$(FM)/$La_{0.6}Ca_{0.4}FeO_3$(AF) superlattices shows that the development of exchange biasing is not a common property in AF/FM perovskite multilayers. The major differences between the two systems are: (i) the drastic increase of magnetization (Fig. 4) in FC curves is not observed at low temperatures in Ref. 3, (ii) the maximum resistivity in Ref. 3 appears at the FM T_c (about 240 K) and not at a much lower temperature ($T_B\approx 70$ K), as in our case. It is reasonable to assign such differences in the chemical composition of the atomic planes at the AF/FM interface. Thus, in Ref. 3, Fe substitutes at the interfaces for Mn as Fe^{3+} and, as in bulk Fe-doped manganites,[27,28] might remain AF coupled to the Mn host lattice of the FM $La_{0.6}Ca_{0.4}MnO_3$ layer.

In our case, the compositional modulation that occurs at the $La_{1-x}Ca_xMnO_3$ interfaces is important because the type of magnetic interactions is defined by the competition between the double-exchange FM coupling and the AF superexchange interactions.[14,15] Geometrical (topological) roughness and interdiffusion between adjacent atomic planes with $x=1/3$ and 2/3 stoichiometries produces an artificial change of concentration to $x\approx 0.5$ at the interfaces. Thus the sequence of magnetic phase transitions might be altered at low temperature in regions with $La_{1/2}Ca_{1/2}MnO_3$ stoichiometry. Bulk measurements[10,29] at $x\approx 0.5$ composition show that the high-temperature FM-conducting phase is followed by a charge ordering transition, resulting in an AF insulator below 120 K. Furthermore, a recent theoretical study[30] shows that the charge ordering observed in 50% doped manganites corresponds to an unusual AF-spin ordering, which exhibits a unique electronic structure with a band-insulator behavior. As a result,[30] strong anisotropy of short-range double-exchange interactions is formed at the charge ordering transition. Since both the T_B and the exchange anisotropy fields appear at about 70 K, that is well below the low-temperature magnetic phase transition for bulk $La_{1/2}Ca_{1/2}MnO_3$, it is reasonable to assume that the appearance of exchange biasing depends on the magnetic ordering of interfacial atomic planes inside an interface volume with $x\approx 0.5$ doping. This interface boundaries define a critical volume where thermal-activation energy becomes less than the low-temperature magnetic energy of $La_{1/2}Ca_{1/2}MnO_3$ at a certain T_B value. Consequently, nearly perfect interfaces (small roughness) will correspond always to the same interface volume with $x\approx 0.5$, giving the same T_B. Since the interface volume with $x\approx 0.5$ doping is fixed for all thicknesses of AF ($x=2/3$) or FM ($x=1/3$) layers, this model is consistent with the observed independence of T_B on t_{AF} or t_{FM}.

In summary, we have shown that the exchange-biasing field increases and the T_c decreases with increasing t_{AF}. The maximum H_{EB} is observed for the 6/3 sample, whereas interface scattering effects give rise to substantial CMR at a

blocking temperature T_B of about 70 K in samples with thicker t_{FM}. The CMR becomes optimum at the 3/6 sample. Zero-field-cooling and field-cooling magnetic measurements reveal that T_B is independent from the FM and the AF layer thickness, indicating that compositional modulation at the $La_{1-x}Ca_xMnO_3$ interfaces is of key importance to the exchange-biasing mechanism in La–Ca–Mn–O based multilayers.

[1] G. Q. Gong, A. Gupta, G. Xiao, P. Lecoeur, and T. R. McGuire, Phys. Rev. B **54**, R3742 (1996).
[2] M. Sahana, M. S. Hedge, V. Prasad, and S. V. Subamanyam, J. Appl. Phys. **85**, 1058 (1999).
[3] M. Izumi, Y. Murakami, Y. Konishi, T. Manako, M. Kawasaki, and Y. Tokura, Phys. Rev. B **60**, 1211 (1999).
[4] K. R. Nikolaev, A. Bhattachrya, P. A. Kraus, V. A. Vas'ko, W. K. Cooley, and A. M. Goldman, Appl. Phys. Lett. **75**, 118 (1999).
[5] B. Wiedenhorst, C. Höfener, Y. Lu, J. Klein, L. Alff, R. Gross, B. H. Freitag, and W. Mader, Appl. Phys. Lett. **74**, 3636 (1999).
[6] C. Kwon, K.-C. Kim, M. C. Robson, J. Y. Gu, M. Rajeswari, T. Venkatesan, and R. Ramesh, J. Appl. Phys. **81**, 4950 (1997).
[7] K. Ghosh, S. B. Ogale, S. P. Pai, M. Robson, E. Li, I. Jin, Zi-wen Dong, R. L. Greene, R. Ramesh, T. Vankatesan, and M. Johnson, Appl. Phys. Lett. **73**, 689 (1998).
[8] R. Cheng, K. Li, S. Wang, Z. Chen, C. Xiong, X. Xu, and Y. Zhang, Appl. Phys. Lett. **72**, 2475 (1998).
[9] I. Panagiotopoulos, C. Christides, M. Pissas, and D. Niarchos, Phys. Rev. B **60**, 485 (1999).
[10] A. J. Millis, Nature (London) **392**, 147 (1998).
[11] W. Prellier, M. Rajeswari, T. Venkatesan, and R. L. Greene, Appl. Phys. Lett. **75**, 1446 (1999).
[12] J. Nogues and I. K. Schuller, J. Magn. Magn. Mater. **192**, 203 (1999).
[13] T. C. Schulthess and W. H. Butler, Phys. Rev. Lett. **81**, 4516 (1998); J. Appl. Phys. **85**, 5510 (1999).
[14] M. Hennion, F. Moussa, J. Rodriguez-Carvajal, L. Pinsard, and A. Revcolevschi, Phys. Rev. B **56**, R497 (1997).
[15] J. B. Goodenough, J. Appl. Phys. **81**, 5330 (1997).
[16] J. H. Underwood and T. W. Berbee, Jr., Appl. Opt. **20**, 3034 (1981).
[17] R. A. Rao, D. Lavric, T. K. Nath, C. B. Eom, L. Wu, and F. Tsui, Appl. Phys. Lett. **73**, 3294 (1998).
[18] J. Mattson, R. Bhadra, J. B. Ketterson, M. Brodsky, and M. Grimsditch, J. Appl. Phys. **67**, 2873 (1990).
[19] O. Allegraza and M.-M. Chen, J. Appl. Phys. **73**, 6218 (1993).
[20] R. Jungblut, R. Coehoorn, M. T. Johnson, J. van de Stegge, and A. Reinders, J. Appl. Phys. **75**, 6659 (1994).
[21] H. S. Wang, Q. Li, K. Liu, and C. L. Chien, Appl. Phys. Lett. **74**, 2212 (1999).
[22] W. Stocklein, S. S. P. Parkin, and J. C. Scott, Phys. Rev. B **38**, 6847 (1988).
[23] Y. K. Kim, K. Ha, and L. L. Rea, IEEE Trans. Magn. **31**, 3823 (1995).
[24] K. Takano, R. H. Kodama, A. E. Berkowitz, W. Cao, and G. Thomas, Phys. Rev. Lett. **79**, 1130 (1997).
[25] K. P. Below, in *Magnetic Transitions* (Boston Technical, Massachusetts, 1965).
[26] M. T. Fernandez-Diaz, J. L. Martinez, J. M. Alonso, and E. Herrero, Phys. Rev. B **59**, 1277 (1999).
[27] K. H. Ahn, X. W. Wu, K. Liu, and C. L. Chien, Phys. Rev. B **54**, 15299 (1996).
[28] A. Simopoulos, M. Pissas, G. Kallias, E. Devlin, N. Moutis, I. Panagiotopoulos, D. Niarchos, C. Christides, and R. S. Sontagg, Phys. Rev. B **59**, 1263 (1999).
[29] P. Schiffer, A. P. Ramirez, W. Bao, and S.-W. Cheong, Phys. Rev. Lett. **75**, 3336 (1995).
[30] I. V. Solovyev and K. Terakura, Phys. Rev. Lett. **83**, 2825 (1999).